Available online at www.sciencedirect.com
ScienceDirect
Scripta Materialia 63 (2010) 560–563
Scripta MATERIALIA
www.elsevier.com/locate/scriptamat

Evolution of microstructural homogeneity in copper processed by high-pressure torsion

X.H. An,[a] S.D. Wu,[a] Z.F. Zhang,[a,*] R.B. Figueiredo,[b] N. Gao[b] and T.G. Langdon[b,c]

[a] *Shenyang National Laboratory for Materials Science, Institute of Metal Research, Chinese Academy of Sciences, 72 Wenhua Road, Shenyang 110016, PR China*

[b] *Materials Research Group, School of Engineering Sciences, University of Southampton, Southampton SO17 1BJ, UK*

[c] *Departments of Aerospace & Mechanical Engineering and Materials Science, University of Southern California, Los Angeles, CA 90089-1453, USA*

Received 24 April 2010; revised 16 May 2010; accepted 21 May 2010
Available online 26 May 2010

Disks of coarse-grained pure Cu were processed by high-pressure torsion (HPT) and the microhardness and microstructural parameters were used to reveal the evolution of homogeneity. It is shown that the microstructures at the centers of the disks are significantly refined by HPT and an essentially homogeneous microstructure is achieved at strains above ~15. An analysis demonstrates that microstructural homogeneity is achieved most readily in materials having either high or low, rather than intermediate, stacking fault energies.

Keywords: Copper; High-pressure torsion; Homogeneity; Microhardness

Severe plastic deformation (SPD) has been widely applied to synthesize bulk materials with ultrafine-grained structures [1]. Various SPD techniques are available including equal-channel angular pressing (ECAP) [2], high-pressure torsion (HPT) [3], accumulative roll-bonding [4] and dynamic plastic deformation [5]. However, processing by HPT is especially attractive because it generally produces significantly smaller grains and a higher fraction of high-angle grain boundaries (HAGBs).

An important limitation in HPT is that the imposed strain varies across the sample. The shear strain in HPT, γ_{HPT}, is given by the relationship [6,7]:

$$\gamma_{HPT} = \frac{2\pi Nr}{h}, \quad (1)$$

where r and h are the radius and height (or thickness) of the disk, respectively, and N is the number of revolutions. Following from Eq. (1), the shear strain in the center of the disk is zero and the strain increases linearly with radius. Several investigations have used microhardness measurements to evaluate the extent of any microstructural evolution occurring in HPT, and the results from these experiments are mutually consistent [8–15]. All results reveal a gradual evolution towards a reasonably homogeneous distribution of microhardness values with increasing pressure and/or increasing strain. This evolution has been effectively modeled using strain gradient plasticity [16]. Nevertheless, no information is available to date concerning the significance of the stacking fault energy (SFE), although it is reasonable to anticipate the SFE plays a critical role because it influences the rate of recovery within the material.

The present investigation was initiated to provide information on the microstructural evolution occurring in coarse-grained pure Cu during processing by HPT. The objectives of the investigation are twofold. First, to provide comprehensive information on the hardness and microstructures for pure Cu processed by HPT. Second, to compare the results with earlier data for various face-centered cubic (fcc) materials processed by HPT and to seek a correlation by incorporating the SFE into the analysis.

The investigation used Cu of 99.97% purity with an initial average grain size of ~57 μm; detailed information about this material was provided previously [17]. Disks were prepared with diameters of 10 mm and thicknesses of ~0.85 mm, and these disks were processed by HPT using the experimental facility and procedure described previously [18,19]. The disks were processed through one, two and five revolutions under an imposed pressure of 6.0 GPa. Following HPT, all samples were mechanically ground and electropolished as described earlier [17] and Vickers microhardness (Hv) measurements were taken with a load of 0.98 N maintained for

* Corresponding author. Tel.: +86 24 23971043; e-mail: zhfzhang@imr.ac.cn

1359-6462/$ - see front matter © 2010 Published by Elsevier Ltd. on behalf of Acta Materialia Inc.
doi:10.1016/j.scriptamat.2010.05.030

10 s using an LM247AT microhardness tester. As depicted schematically in Figure 1a, measurements across the diameter were taken at positions separated by 0.3 mm up to a distance of 2.1 mm on either side of the center and at separations of 0.5 mm thereafter. Using electron backscatter diffraction (EBSD), detailed microstructural observations were undertaken at the centers, at the half-radius positions ((1/2)R) and near the edges (1R) of each HPT disk, where R is the disk radius. The EBSD investigations were undertaken using a LEO SUPRA35 scanning electron microscope with map step sizes of 0.5 μm for the central regions of the disks after one and two revolutions, 0.08 μm for the central region after five revolutions and 0.05 μm for the (1/2)R and 1R positions after one revolution. At least three maps were scanned in the selected regions for each condition to provide a high level of accuracy. The microstructural evolution was recorded using Channel 5 software (HKL Technology) [20] and analyzed to give the average grain size, the fraction of HAGBs having misorientation angles of >15° and the average misorientation angle, θ_{av}.

The average values of Hv across the diameters of each disk are shown in Figure 1b, where CG denotes the initially unprocessed hardness. Several trends are visible from inspection of Figure 1b. First, the microhardness increases by a factor of approximately 2 after one-revolution HPT. The increased Hv in the central regions can be attributed to the gradient in hardness, since the ideal center of the sample with non-zero strain is only an infinitesimal point [21]. Second, there is a significant variation in the size of the error bars across the disk diameters: specifically, the error bars are larger in the central region and decrease with increasing numbers of revolutions, thereby indicating a gradual transition to microstructural uniformity after larger numbers of revolutions. Third, the low values of Hv in the central region increase in subsequent strains and ultimately, after five revolutions, all Hv values are reasonably uniform across the disk. Fourth, the Hv values at the outer periphery undergo no significant change with increasing numbers of revolutions, which is similar to earlier data for an Al-6061 alloy [12]. Moreover, the relationship between the equivalent von Mises strain ε_{VM} in HPT and the flow stress is shown in Figure 1c. It is apparent that significant strain hardening takes place only at the lower strains and, as shown in the inset, the flow stress is essentially constant at equivalent strains larger than about 15.

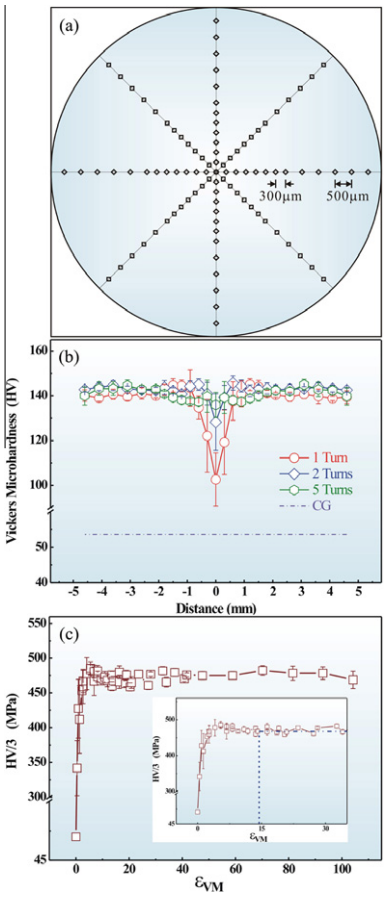

Figure 1. (a) Schematic illustration of the procedure for microhardness measurements across the diameters of disks after HPT; (b) the average Vickers microhardness, Hv, versus the distance from the center of the disk and (c) the stress–strain relationship of Cu after HPT: the inset shows the stabilization at a strain of ~15.

The distribution of crystallographic orientations may be readily evaluated through inverse pole figures by using EBSD as shown in Figure 2a–e and the colors correspond to different orientations in the inverse pole figure as shown in Figure 2f. Inspection of Figure 2a shows that the original grains are clearly discernible in the center after one revolution and the density of low-angle boundaries (LAGBs) is very high. There are fluctuations in the orientations within the grains and there are larger changes in the orientations adjacent to the grain boundaries and near the triple junctions. These orientation fluctuations are more obvious in the central region after two revolutions, as shown in Figure 2b, although many of the coarse original grains are visible. These distorted crystallographic orientations originate from dislocation activities which lead to the formation of LAGBs [22]. After five revolutions in Figure 2c, the microstructure at the center is significantly refined; the original coarse grains are invisible but the density of LAGBs remains high.

It is well documented that grain refinement of pure Cu in SPD processing, as in ECAP, is dominated by the accumulation, interaction, tangling and spatial rearrangement of dislocations [23]. It is apparent also from Figure 2 that microstructural evolution occurs differently outside of the central region. At the (1/2)R position after one revolution where the equivalent strain is ~15, as shown in Figure 2d, the microstructure is fairly homogeneous and well refined with an average grain size of ~140 nm. This grain size is smaller than the grain sizes measured by transmission electron microscopy in pure Cu processed by ECAP (~270 nm after 10 passes [24] and ~180 nm after 12 and 16 passes [23]) and by HPT at the lower pressure of 2.0 GPa (~200 nm after one revolution [25]). However, it is identical to the grain size of ~140 nm reported in the outer region of a disk of Cu processed by HPT for five revolutions under the same pressure [26] and it is similar to the grain size of ~150 nm reported in Cu after five revolutions at 5.0 GPa [27]. A similar structure is visible in Figure 2e at the 1R position after one revolution, thereby suggesting that a saturation grain size is achieved at a strain of $\varepsilon_{VM} \approx 15$. The microstructures at the (1/2)R and 1R positions after two and five revolutions are similar to those in Figure 2d and e.

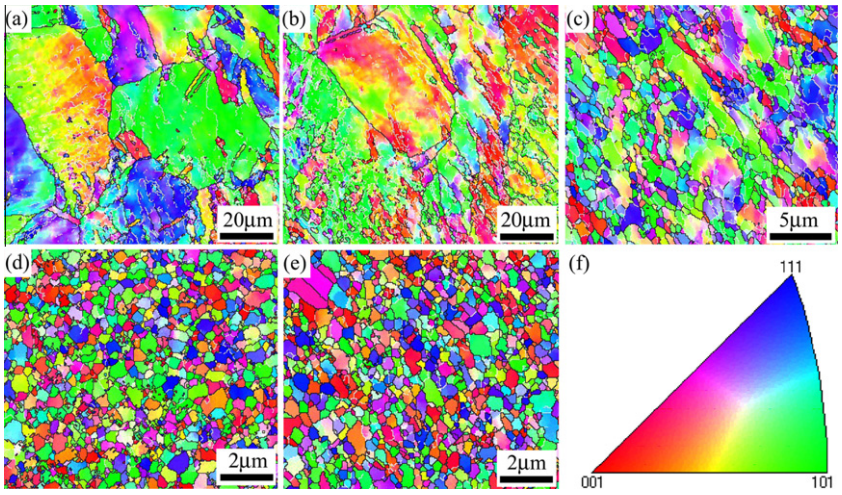

Figure 2. Microstructures in the disks at selected positions after different numbers of revolutions: (a–c) central areas of the disk after one, two and five revolutions, respectively; (d and e) (1/2)*R* position and 1*R* position, respectively, after one revolution and (f) the inverse pole figure.

Figure 3 presents a detailed summary of the microstructural parameters including (a) the average grain size, (b) the relative fraction of HAGBs and (c) the θ_{av}. The average grain size in the central region decreases with increasing numbers of revolutions and after five revolutions it is comparable to, but higher than, the grain size of ~140 nm achieved at the (1/2)*R* and 1*R* positions after one revolution. Concurrently, the fraction of HAGBs and the values of θ_{av} in the central regions increase with increasing numbers of revolutions. Although the grain sizes are fairly similar at the three selected positions after five revolutions, the fraction of HAGBs and the θ_{av} remain significantly lower in the central region. This implies that microstructural evolution is not complete even after five revolutions of HPT despite the very significant grain refinement. The values of the HAGB fraction (~75%) and θ_{av} (~33°) at the (1/2)*R* and 1*R* positions are essentially constant from one to five revolutions and the former value is higher than the fraction of ~62% of HAGBs in Cu processed by 24 passes of ECAP [28].

The presence of inhomogeneity within the Cu disk is different from the homogeneity achieved in high-purity Al after processing by HPT through five revolutions [9]. This suggests that the development of homogeneity is dependent upon the rate of recovery within the material and therefore upon the SFE. In practice, the SFE determines not only the recovery rate but also the deformation mechanisms which influence the homogeneity evolution within fcc materials [29–33]. In order to evaluate the level of microstructural homogeneity achieved in fcc materials, it is convenient to define a hardening parameter $((HV_R - HV_C)/HV_R)$, where HV_R and HV_C represent the values of Hv at the 1*R* position and near the central region, respectively. Using the experimental data obtained after five-revolutions HPT at RT in the present investigation and other reports for different fcc materials [9,10], Figure 4a plots the hardness parameter against the normalized SFE, γ/Gb, where *G* is the shear modulus and *b* is the Burgers vector, and Figure 4b shows an additional plot where the von Mises equivalent strain for an apparently homogeneous microstructure in HPT is also plotted against γ/Gb [9,10,22,34]. The two plots in Figure 4a and b signal that a uniform microstructure is attained more easily in fcc materials that have either a high

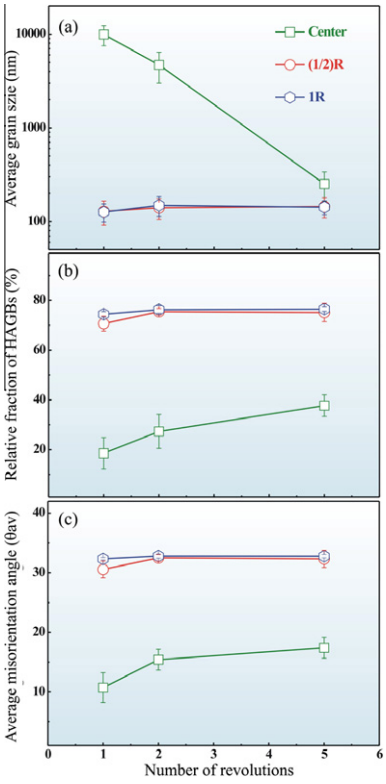

Figure 3. Evolution of microstructure parameters with increasing numbers of revolutions: (a) the average grain size; (b) the fraction of HAGBs and (c) the θ_{av}.

or a low SFE. This conclusion is also consistent with recent investigations using ECAP [30–33].

In addition, it is known that increasing the deformation temperature may achieve a uniform microstructure more readily [22]. In the present analysis the HPT processing was conducted at RT where the homologous temperatures are in the same range for all selected fcc materials shown in Figure 4 (from ~$0.3T_m$ for Al to ~$0.2T_m$ for Ni where T_m is the melting temperature). Thus, although the homologous temperature may slightly influence the microstructural evolution [35], the SFE appears to be the most important factor influencing the development of microstructural homogeneity.

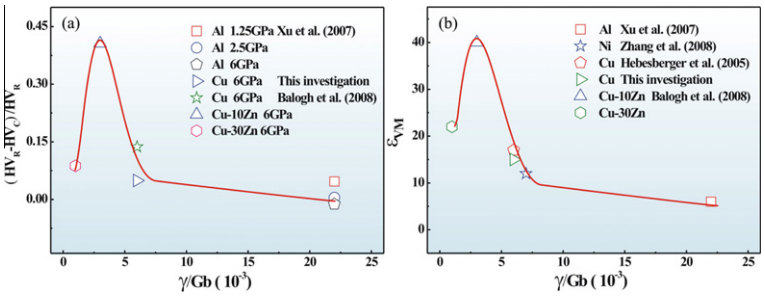

Figure 4. (a) Relationship between the hardness parameter after five revolutions and the SFE [9,10] and (b) relationship between the equivalent strain required to develop a homogeneous microstructure and the SFE [9,10,21,32].

The reason for the apparent dichotomy between high, low and intermediate SFE materials lies in the nature of the dominant deformation process in achieving grain refinement. In the materials with high SFE there is a high rate of recovery and a rapid evolution into a uniform microstructure [9], whereas in the materials with low SFE the recovery occurs slowly because of the significant difficulty of cross-slip, but deformation twinning transforms the homogeneously deformed metals into a fine laminar structure and this is readily fragmented to refine grains [30]. The intersection of twins, secondary twins and shear bands accelerates the formation of a reasonably uniform distribution of nanostructured grains [30–33,36]. Consequently, it appears that the formation of a uniform ultrafine microstructure is most challenging in materials where the rate of recovery is relatively slow and, in addition, the formation of a homogeneously twinned structure is difficult [17,31].

In summary, experiments on pure Cu demonstrate an evolution in microstructure and microstructural parameters during processing by HPT which is consistent with expectations inferred indirectly from microhardness measurements. Although the microstructures in the central regions are significantly refined with increasing numbers of revolutions, and reach an essentially homogeneous condition at strains above ~15, the fraction of HAGBs and the θ_{av} lag behind the evolution achieved in the outer regions of the disks. A comparison with other experimental data suggests that microstructural homogeneity is achieved most readily in the fcc materials having high or low, rather than intermediate, SFEs.

This work was supported by the Innovation Fund for Graduate Students of IMR-CAS and the National Natural Science Foundation of China (NSFC) under Grant Nos. 50841024, 50890173 and 50931005. Z.Z.F. acknowledges financial support from the National Outstanding Young Scientist Foundation under Grant No. 50625103 and the Royal Society of the UK under International Joint Project No. JP871294.

[1] R.Z. Valiev, R.K. Islamgaliev, I.V. Alexandrov, Prog. Mater. Sci. 45 (2000) 103.
[2] R.Z. Valiev, T.G. Langdon, Prog. Mater. Sci. 51 (2006) 881.
[3] A.P. Zhilyaev, T.G. Langdon, Prog. Mater. Sci. 53 (2008) 893.
[4] Y. Saito, H. Utsunomiya, N. Tsuji, T. Sakai, Acta Mater. 47 (1999) 579.
[5] Y.S. Li, N.R. Tao, K. Lu, Acta Mater. 56 (2008) 230.
[6] R.Z. Valiev, Yu.V. Ivanisenko, E.F. Rauch, B. Baudelet, Acta Mater. 44 (1996) 4705.
[7] F. Wetscher, A. Vorhauer, R. Stock, R. Pippan, Mater. Sci. Eng. A 387–389 (2004) 809.
[8] A.P. Zhilyaev, G.V. Nurislamova, B.-K. Kim, M.D. Baró, J.A. Szpunar, T.G. Langdon, Acta Mater. 51 (2003) 753.
[9] C. Xu, Z. Horita, T.G. Langdon, Acta Mater. 55 (2007) 203.
[10] L. Balogh, T. Ungár, Y.H. Zhao, Y.T. Zhu, Z. Horita, C. Xu, T.G. Langdon, Acta Mater. 56 (2008) 809.
[11] C. Xu, Z. Horita, T.G. Langdon, Acta Mater. 56 (2008) 5168.
[12] C. Xu, Z. Horita, T.G. Langdon, J. Mater. Sci. 43 (2008) 7286.
[13] C. Xu, T.G. Langdon, Mater. Sci. Eng. A 503 (2009) 71.
[14] M. Kawasaki, B. Ahn, T.G. Langdon, Acta Mater. 58 (2010) 919.
[15] C. Xu, Z. Horita, T.G. Langdon, Mater. Trans. 51 (2010) 2.
[16] Y. Estrin, A. Molotnikov, C.H.J. Davies, R. Lapovok, J. Mech. Phys. Solids 56 (2008) 1186.
[17] C.X. Huang, K. Wang, S.D. Wu, Z.F. Zhang, G.Y. Li, S.X. Li, Acta Mater. 54 (2006) 655.
[18] M. Kawasaki, T.G. Langdon, Mater. Sci. Eng. A 498 (2008) 341.
[19] Y.Z. Tian, X.H. An, S.D. Wu, Z.F. Zhang, R.B. Figueiredo, N. Gao, T.G. Langdon, Scripta Mater. 63 (2010) 65.
[20] F.J. Humphreys, J. Mater. Sci. 36 (2001) 3833.
[21] A. Vorhauer, R. Pippan, Scripta Mater. 51 (2004) 921.
[22] T. Hebesberger, H.P. Stuwe, A. Vorhauer, F. Wetscher, R. Pippan, Acta Mater. 53 (2005) 393.
[23] F. Dalla Torre, R. Lapovok, J. Sandlin, P.F. Thomson, C.H.J. Davies, E.V. Pereloma, Acta Mater. 52 (2004) 4819.
[24] S. Komura, Z. Horita, M. Nemoto, T.G. Langdon, J. Mater. Res. 14 (1999) 4044.
[25] K. Edalati, T. Fujioka, Z. Horita, Mater. Sci. Eng. A 497 (2008) 168.
[26] Z. Horita, T.G. Langdon, Mater. Sci. Eng. A 410–411 (2005) 422.
[27] H. Jiang, Y.T. Zhu, D.P. Butt, I.V. Alexandrov, T.C. Lowe, Mater. Sci. Eng. A 290 (2000) 128.
[28] C.X. Huang, H.J. Yang, S.D. Wu, Z.F. Zhang, Mater. Sci. Forum 584 (2008) 333.
[29] X.H. An, W.Z. Han, C.X. Huang, P. Zhang, G. Yang, S.D. Wu, Z.F. Zhang, Appl. Phys. Lett. 92 (2008) 201915.
[30] S. Qu, X.H. An, H.J. Yang, C.X. Huang, G. Yang, Q.S. Zang, Z.G. Wang, S.D. Wu, Z.F. Zhang, Acta Mater. 57 (2009) 1586.
[31] X.H. An, Q.Y. Lin, S. Qu, G. Yang, S.D. Wu, Z.F. Zhang, J. Mater. Res. 24 (2009) 3636.
[32] S.D. Wu, X.H. An, W.Z. Han, S. Qu, Z.F. Zhang, Acta Mater. Sin. 46 (2010) 257.
[33] X.H. An, Q.Y. Lin, S.D. Wu, Z.F. Zhang, Mater. Sci. Eng. A 527 (2010) 4510.
[34] H.W. Zhang, X. Huang, N. Hansen, Acta Mater. 56 (2008) 5451.
[35] K. Edalati, Z. Horita, Mater. Trans. 51 (2010) 1051.
[36] N.R. Tao, K. Lu, Scripta Mater. 60 (2009) 1039.